第 54 卷第 1 期
2026 年 1 月

硅 酸 盐 学 报
JOURNAL OF THE CHINESE CERAMIC SOCIETY

Vol. 54，No. 1
January，2026

http://jccsoc.cbpt.cnki.net

DOI：10.14062/j.issn.0454-5648.20250274

综 合 评 述

基于注射成型技术制备石英玻璃和复合荧光石英玻璃的研究进展

Moushira A MOHAMED[1]，Mohamed A ALI[1]，刘小峰[2]，邱建荣[1]

(1. 浙江大学极端光学技术与仪器全国重点实验室；浙江大学光电科学与工程学院，杭州 310027；
2. 浙江大学材料科学与工程学院，杭州 310058)

摘 要：纯石英玻璃是一种非常重要的无机材料，具有高透明度、高稳定性、绝缘性和低热膨胀特性等诸多特点，被广泛应用于光子学、微流体等领域。复合荧光粉的石英玻璃(PiSG)可作为光谱转换材料，兼具荧光材料的高发光效率与石英玻璃的优异化学和热稳定性，可用于制造高功率和高稳定的白光 LED。近年来，学者们使用不同的增材制造(AM)技术并结合烧结开发了各种形状的透明石英玻璃及荧光粉复合的石英玻璃。由于这些新的制造方法可以在相对较低的温度(成型温度低于 150 ℃，烧结温度低于 1300 ℃)下实现石英玻璃产品的制备，近年来关注度日益提高。在 AM/烧结技术中，注塑成型(IM)/烧结技术在能耗及制造成本等方面优势显著，适合大规模工业生产形状复杂、尺寸定制的石英基玻璃材料。本文重点介绍了基于 IM/烧结技术制造石英基玻璃材料的最新进展。此外，还概述了注塑成型石英基玻璃材料在微流体和光子学领域的应用，最后讨论了注塑成型玻璃基复合材料的挑战和未来研究方向。

关键词：石英玻璃；注塑成型；荧光粉；稳定的照明设备；固态照明
中图分类号：TQ175　　**文献标志码**：A　　**文章编号**：0454–5648(2026)01–0271–15
网络出版时间：2025–12–04

1 Introduction

Among all glass families (*e.g.*, metallic, organic, inorganic, and organic-inorganic hybrids), fused silica glass is characterized by the most stable and non-toxic network [1–2]. Silica glass is an amorphous 3D network, consisting of Si–O bonds, where each silicon atom is covalently bonded to four oxygen atoms in a tetrahedral arrangement. The oxygen atoms act as bridging units, linking two silicon atoms and forming a highly cross-linked and rigid 3D network. This unique structure gives silica glass exceptional physicochemical properties, such as high-transparency, outstanding chemical and thermal stabilities, non-toxicity, high hardness, low thermal and electrical conductivities, and minimal thermal expansion [1]. These advantages enable silica glass to be an ideal material for various applications (*e.g.*, medicine, microfluidics, and photonics) [3–5]. In industrial production, fused silica glass is typically fabricated using melting-quenching technique, which requires extremely high-temperatures (~2000 ℃), making the process energy-intensive [2, 6–7]. For example, centimeter-scale silica glass with different 3D geometries is produced *via* a selective laser melting (SLM) and precision glass molding (PGM) technologies [8–9]. Meanwhile, microscale silica structures are often fabricated using a surface wet etching (SWE) approach [10]. However, each method possesses limitations: PGM, while capable of producing complex, large and high-precision components, it suffers from low-to-medium productivity and high-energy consumption. On the other hand, SLM produces glass with poor precision, high-surface roughness, and slow printing speeds. Furthermore, SWE technique requires additional surface polishing to achieve smoothness and it has limitations in terms of shape complexity, precision, and production rate. Despite the commercial availability of fused silica glass, the manufacturing of high-quality silica glass with high-throughput, low shaping temperatures, minimal energy consumption and low cost, especially at micrometer and centimeter scales—remains a challenge for SLM, PGM, and SWE techniques [8–10]. The primary obstacle is associated with the high-melting temperature of silica, which complicates shaping processes and increases energy demands.

收稿日期：2025–04–15。　修订日期：2025–04–23。
基金项目：国家重点研究计划(2024YFB4607400)；国家自然科学基金(W2442019，52050410326，52161135109，12104397，52432001)。
第一作者：Moushira A MOHAMED(1987—)，女，博士研究生。
通信作者：邱建荣(1964—)，男，博士，教授。

Received date: 2025–04–15.　**Revised date:** 2025–04–23.
First author: Moushira A MOHAMED (1987–), female, Doctoral candidate.
E-mail: 12230102@zju.edu.cn
Correspondent author: QIU Jianrong (1964–), male, Ph. D., Professor.
E-mail: qjr@zju.edu.cn

To address these technical challenges, researchers have recently developed innovative methods that facilitate the fabrication of complex-structured silica glass at low temperatures, achieving high-quality and productivity suitable for commercial applications [11]. These methods involve combining amorphous silica nanopowder with different types of photopolymers or thermopolymers to create silica-polymer nanocomposites. The resultant composites are then structured into intricate micro and centimeter-sized components using a heat (< 150 ℃) or an ultraviolet (UV) light through different additive manufacturing (AM) techniques [12]. The printed silica-polymer nanocomposites with designed structure are called as green parts. Remarkably, after undergoing a series of thermal debinding processes at 600 ℃ to remove the polymeric binders from the green parts, followed by sintering at temperatures below 1300 ℃, the amorphous silica nanoparticles are transformed into a bulk glass. It is noteworthy that the preparation of silica-polymer nanocomposites enhances the shaping of complex-structured silica glass at low temperatures with a high-precision. This is due to the sufficient polymer content in nanocomposites that allows for molding through various AM techniques [13]. Furthermore, the densification of amorphous silica nanoparticles into bulk glass during sintering process at temperatures below 1300 ℃ significantly reduces the needed energy for silica glass industry, which typically requires 2000 ℃ for glass melting. Overall, AM/sintering approaches enable the production of high-quality silica glass with complex geometries that cannot be achieved through the conventional methods such as SLM, PGM, and SWE [12].

To fabricate centimeter-sized silica glass, several structuring techniques such as soft replication, direct ink writing (DIW), thermal imprinting, laser ablation, mechanical subtractive machining, origami, fused deposition modeling (FDM), and injection molding (IM) were employed to customize green parts with desired shapes, resulting in high-quality and transparent silica glass after the debinding and sintering processes [14–19]. However, the production of micro-sized silica glass was accomplished through various methods, including stereolithography (SLA)/sintering, two-photon lithography (TPL)/sintering, and microscale computed axial lithography (μCAL)/sintering technologies [20–22]. By utilizing AM/sintering techniques, silica glasses in both micro and centimeter sizes have been successfully manufactured with high-transparency and intricate designs such as woodpile scaffolds, 3D towers, skeletal gyroid lattices, hierarchical lattice structures, hollow castle gates, and microlenses. The as-prepared silica-polymer nanocomposites were easily shaped using AM method at temperatures below 150 ℃ then converted into bulk silica glass products at low sintering temperatures (<1300 ℃) [11]. Additionally, various silica-organic photopolymers, including polyhedral oligomeric silsesquioxane, hydrogen silsesquioxane, and poly(dimethylsiloxane) served as photoresins for 3D printing through the TPL technique, which was subsequently converted into silica glass at low sintering temperatures (< 900 ℃) [23–25]. The application of AM and sintering process was not limited to the single-component silica glass, but it allowed for the fabrication of multicomponent glasses [26–30]. By comparing the reported AM/sintering techniques, IM/sintering technique presents a novel approach for the manufacturing of centimeter-sized silica glass with complex structures, varying sizes and precise specifications, meeting the industry's demands for high productivity and low energy consumption [11, 19]. A significant limitation of other AM/sintering technique is the lengthy printing duration, which ranges from several hours to a day, depending on the size and complexity of the printed object [11–12, 19]. In contrast, TPL/sintering technique could produce intricate silica glass microstructures with resolutions between 100–200 nm, demonstrating significantly higher resolution than those achieved through SLA/sintering and μCAL/sintering technique, which typically yield resolutions around 50 μm [11].

Silica glass is a highly robust material for serving as a stable matrix for luminescent inorganic phosphors [31–35]. This is attributed to its excellent transparency in the visible (Vis) and near-infrared (NIR) regions, along with its remarkable chemical and thermal stabilities, and low thermal conductivity. Inorganic phosphors, which include oxides, halides, chalcogenides, and nitrides, are a category of luminescent materials capable of emitting light efficiently across spectral ranges from UV light to NIR light [36]. Due to their high internal quantum efficiency (IQE) and robust stability, these luminescent phosphors find several applications in diverse areas such as lighting, sensing, optical thermometry, photovoltaic cell, and bioimaging [37]. In the lighting applications, high-power phosphor-converted light-emitting-diodes (pc-LEDs) are produced by integrating a transparent, efficient, blue-excitable phosphor converter with a blue InGaN chip (typically emitting at 420–460 nm), resulting in the generation of high-power and bright Vis-NIR light [32, 38]. To ensure light extract from the phosphor converter, luminescent phosphors are usually embedded in silicone resin or glass matrix, or synthesized as single crystals or transparent ceramics [39–40].

Given that glasses exhibit superior chemical and thermal stabilities compared to silicone resin, phosphor-in-glass (PiG) is often favored as a spectral converter. Furthermore, PiG is significantly more cost-effective than single crystals and transparent ceramics. Consequently, luminescent phosphor powders have been integrated into various oxide glasses such as borates, phosphates, tellurites, borosilicates and pure silica glasses, to create transparent PiG with effective luminescent characteristics [32, 41]. Among several PiG

color converters, phosphor-in-silica glass (PiSG) stands out as the most effective spectral converter, as it combines the advantages of luminescent phosphors (*i.e.*, high IQE) with the beneficial properties of silica glass (*i.e.*, high-chemical and thermal stabilities) [31–33]. The incorporation of luminescent phosphor into silica glass enhances the lifetime of LED devices and facilitates the production of high-power LEDs. Recent studies have demonstrated the creation of transparent PiSG converters using spark plasma sintering (SPS), SLA/sintering, and IM/sintering techniques [31–35, 42]. Among these methods, IM/sintering technique is considered as a cost-effective and energy-efficient solution for large-scale production of PiSG with desired designs, thereby supporting the development of high-power, low-cost, and stable pc-LEDs [19, 33–35].

Owing to the significance of IM/sintering technique in the efficient manufacturing of glass and crystal-glass composites, this review aims to summarize the latest advancements in the production of transparent silica glass and PiSG composites through IM/sintering technique for lighting applications. We first provided a detailed discussion of the IM/sintering process for the high-throughput fabrication of transparent silica glass, including the impact of debinding processes on the quality of the glass. Subsequently, we discussed the production of PiSG composites and their potential applications in photonics. Finally, we addressed the existing challenges and outline the future prospects for the fabrication of glass and PiSG using IM/sintering technique.

2 Injection-molded silica glass

2.1 Fabrication of complex silica glass components *via* IM technology

IM is a manufacturing technique that involves the injection of molten material into a mold to create designed parts. This process is characterized by its versatility and efficiency, makes it a popular choice in numerous industries for the mass production of high-quality components [43]. Therefore, IM is predominantly utilized for fabricating plastics, metal, ceramic, and glass products [19, 43–44]. The IM process is distinguished by its high-production rates and its ability to create intricate shapes at a low cost. To produce silica glass, the IM technique has been adapted specifically for the creation of glass components, aligning with the demands of the large-scale glass industry [19, 45].

In 2021, Mader *et al*. utilized IM for the pre-shaping of a silica-plastic nanocomposite intended for the high-throughput production of silica glass [19, 45]. The authors used polyethylene glycol (PEG, 400–4000 g/mol) and polyvinyl butyral (PVB, 11 000–30 000 g/mol) as thermoplastic materials and amorphous silica nanopowder (particle size of 50–100 nm) as the silica source. As shown in Fig. 1, PEG, PVB and silica nanopowder were mixed in the presence of tetrahydrofuran. After homogenizing the mixture, the solvent was removed by evaporation, resulting in the formation of a solid silica-thermoplastic nanocomposite. At 130 ℃, this silica-thermoplastic feedstock was plasticized then extruded using a double twin screw extruder, forming the final feedstock as granules with a high silica loading of 60% (in volume fraction). The molten silica-thermoplastic nanocomposite at 130 ℃ demonstrated a viscosity below 1000 Pa·s, which was necessary for successful IM process [43]. Subsequently, the as-prepared silica-thermoplastic granules were melted then injection-molded at a moderate temperature of 130 ℃ and injection pressures of 700–1000 bar, resulting in the formation silica-thermoplastic green parts with the designed shape and size. After molding process, two step debinding processes were performed to remove the PEG and PVB binders from the green part and to form the polymer-free samples (*i.e.*, brown parts). At first, a green part (< 2 mm thickness) was immersed in water at 40 ℃ for 3 h to remove more than 95% (in mass fraction) of PEG binder. For green parts with larger thicknesses, the water debinding duration should be increased to eliminate the majority of PEG. In the second debinding step (called as thermal debinding), the remained PEG and PVB in the water debound green parts, were decomposed through heating the samples in air at 270, 460 ℃, and 600 ℃ for 1 h at each temperature (heating rate of 1 ℃/min). Finally, the resultant brown part was sintered in a vacuum at 1300 ℃ for 3 h to obtain the high-quality and transparent silica glass. The total time to produce injection-molded silica glass with a 2 mm thickness is 24 h, including all the IM/debinding/sintering steps [19, 33–35, 45]. However, the process duration for larger samples is increased because of the increase of water debinding period to remove PEG from green parts.

To demonstrate the high-throughput production of IM technology, the authors prepared more than 200 parts with complex shape within only 18 min (Fig. 2a), at a molding time of 5 s/piece. In addition, by using various molds, different transparent silica glasses with complex structures and high-precision were fabricated *via* IM/sintering technique as shown in Fig. 2b. While the molding rate can be as high as 5 s/piece, this technique allows for high-throughput fabrication of complex green bodies. This molding rate was the fastest among all AM processes that have been employed to fabricate silica glass [11–12]. The injection-molded silica glasses exhibited excellent optical properties, with a transparency of 90% and a low surface roughness of 3.74 nm. Additionally, the results showed that the density of the injection-molded silica glass is 2.204 g/cm^3, which was close to that of the commercial fused silica glass. A key advantage of the IM/sintering method was its environmental sustainability. Unlike thermal decomposition, the water debinding process allows for the recycling of PEG, thus reducing environmental pollution. Furthermore, the silica-thermoplastic feedstock consists of non-toxic, widely

available polymers and silica powders, ensuring safer processing. Moreover, the shaping process was performed at a moderate temperature of 130 ℃, while the conversion to transparent fused silica glass required a sintering process at 1300 ℃, which was significantly lower than the melting temperature of silica glass (>2000 ℃), thereby reducing energy consumption. These benefits demonstrated that IM/sintering is a sustainable, energy efficient, and mass-productivity method for the manufacturing of high-quality silica glass, making it highly promising for industrial and commercial applications.

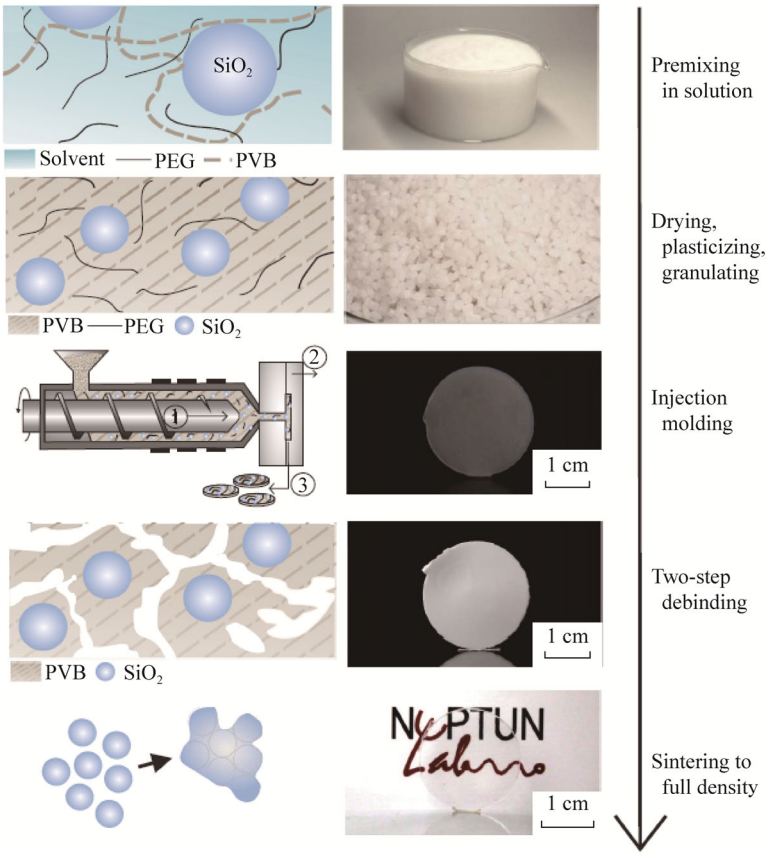


Fig. 1 Schematic representation of the fabrication of silica glass using IM/sintering technique [19]

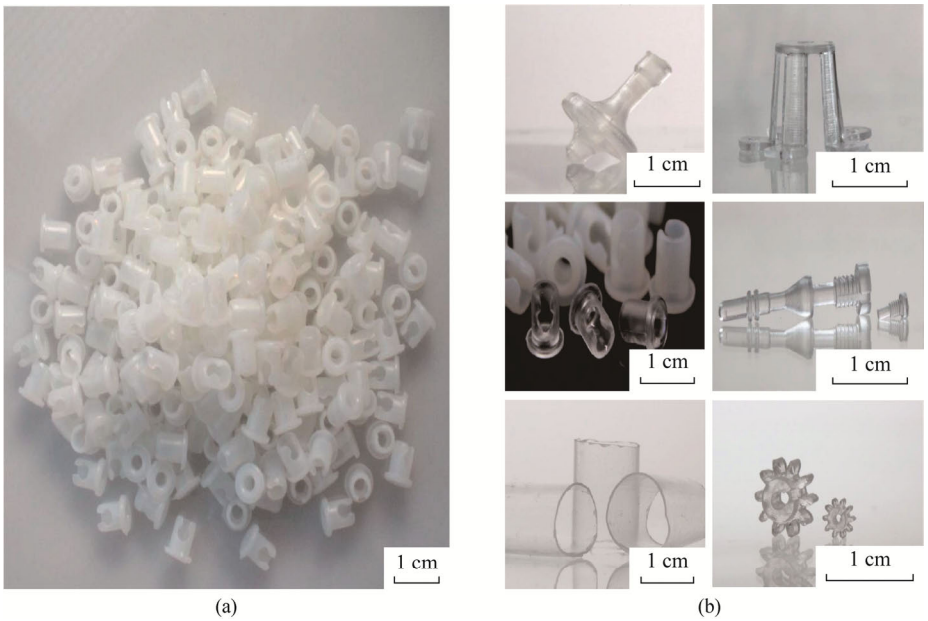


Fig. 2 (a) Photograph for the injection-molded green parts, demonstrating the high-throughput production of IM technique; (b) Photographs for different complex-structured and centimeter-sized silica glasses prepared by IM/sintering technique [19]

In the same report, the authors did not only fabricate a centimeter-sized silica glass *via* IM/sintering technique, but also manufactured spherical and cylindrical microlens arrays. This could be occurred through the replication of microlens on the surface of the molded green parts, which formed glassy microlens after performing a series of debinding and sintering. As shown in Fig. 3a–Fig. 3b, the scanning electron microscope (SEM) images confirmed that the replicated microlens possess high-quality with ordered structures. Furthermore, well-resolved refraction pattern was observed when illuminating the cylindrical microlens array with a green laser (532 nm) as shown in Fig. 3c. To embed silica glass in microfluidic application, the authors fabricated an injection-molded fused silica component containing a microfluidic channel structure (*e.g.*, an exemplary serpentine channel) as shown in Fig. 3d. The width and height of the microchannel are 240 μm and 580 μm, respectively. The as-fabricated microfluidic device based on injection-molded silica glass was filled with dyed water (Fig. 3e), confirming the fabrication of closed and leak-proof microfluidics. Although the IM/sintering technique can produce silica glass with different microstructures (*e.g.*, microlens and microchannels) at the surface, the fabrication of more complex micro-structures is challenging, therefore this technique is more appropriate for the centimeter-sized silica glasses with various shapes and high-precision. To fabricate optically active glass, metal nanoparticles, transition metal ions and rare earth ions were introduced into the injection-molded silica glasses, yielding luminescent or strong colored glasses as shown in Fig. 3f. These results suggest that the injection-molded silica glass is promising for novel applications in diverse fields from packing, lighting, optics and microfluidic reactors [4, 23–25, 46].

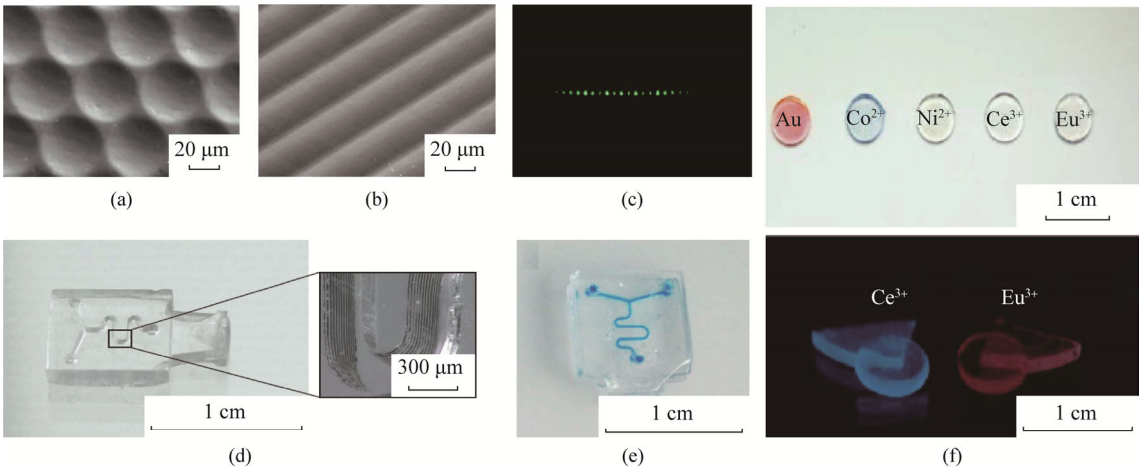


Fig. 3　SEM images of the injection-molded silica glasses containing (a) spherical and (b) cylindrical microlens arrays; (c) The observed refraction pattern when illuminating the cylindrical microlens array with a green laser (532 nm); (d) Injection-molded fused silica component with a microfluidic channel structure; The inset showed a magnification of the channel; (e) Bonded fused silica microfluidic device filled with dyed water; (f) Photographs of the injection-molded silica glass doped with Au nanoparticles, Co^{2+}, Ni^{2+}, Ce^{3+}, and Eu^{3+} ions taken in the daylight (up) and under UV light (down) [19]

2.2　Importance of water debinding process

Researchers have studied the impact of debinding process on the silica glass formation using IM/sintering technique [19, 45, 47]. In 2024, Guo *et al*. revealed that the water debinding process is essential for producing high-quality injection-molded silica glass [45]. They observed that the reduction in the amount of decomposed polymer through water debinding process not only decreases the environmental pollution, but also reduced the formation of cracks in the brown part after thermal debinding. Hence, the quality of injection-molded silica glass was much improved when they employed water/thermal debinding for the green parts. On the other hand, the as-fabricated injection-molded silica glass without water debinding step led to the formation of low quality sample contains many cracks as shown in Fig. 4. In this report, the composition of silica-thermoplastic green part was 20% PEG-20% PVB-60% silica (in mass fraction). This means that the direct thermal debinding of the green parts results in the loss of 40% of their weights, which is relatively high and induce the formation of cracks in the brown part during heating process at 600 ℃. However, after removing PEG by water debinding process at 40 ℃, the decomposed amount of polymers during thermal debinding significantly decreases from 40% to 25% (in mass fraction), prohibiting the formation of cracks in the brown part and thus improve the glass quality.

Water debinding process enhances the packing of silica nanoparticles in the brown parts through the increase in both the surface charge and the molecular structure ordering of silica nanoparticles [45, 47]. This could decrease the number of micro-sized pores in the brown parts and thus facilitate the densification process of silica nanoparticles during sintering (Fig. 5a). As shown in Fig. 5b and Fig. 5c, the molecular structure ordering and

the surface charge of silica nanoparticles in the brown part were examined by a Fourier-transform infrared (FTIR) spectroscopy and a Zeta potential analyzer. The FTIR results indicated that the molecular structure ordering of silica nanoparticles in the brown part is increased after water and thermal debinding, while the nanoparticles in the brown part that prepared only by thermal debinding demonstrated higher disordering (Fig. 5b). This is inferred based on the fact that the absorption resonance peak of SiO_4 units in the prepared brown part by water/thermal debinding becomes sharper compared with that fabricated by thermal debinding only. Additionally, the Zeta potential data showed that the surface charge negativity of silica nanoparticles in the brown part increases with increasing water debinding duration as show in Fig. 5c.

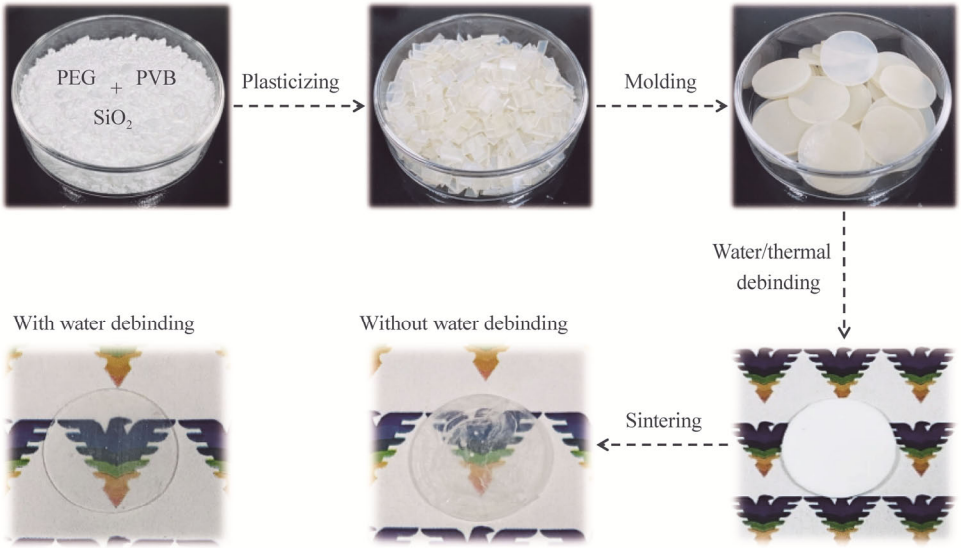


Fig. 4 Schematic illustration of the fabrication of the silica glass using IM and sintering technique, demonstrating the impact of water debinding on the quality of the sintered glass [45]

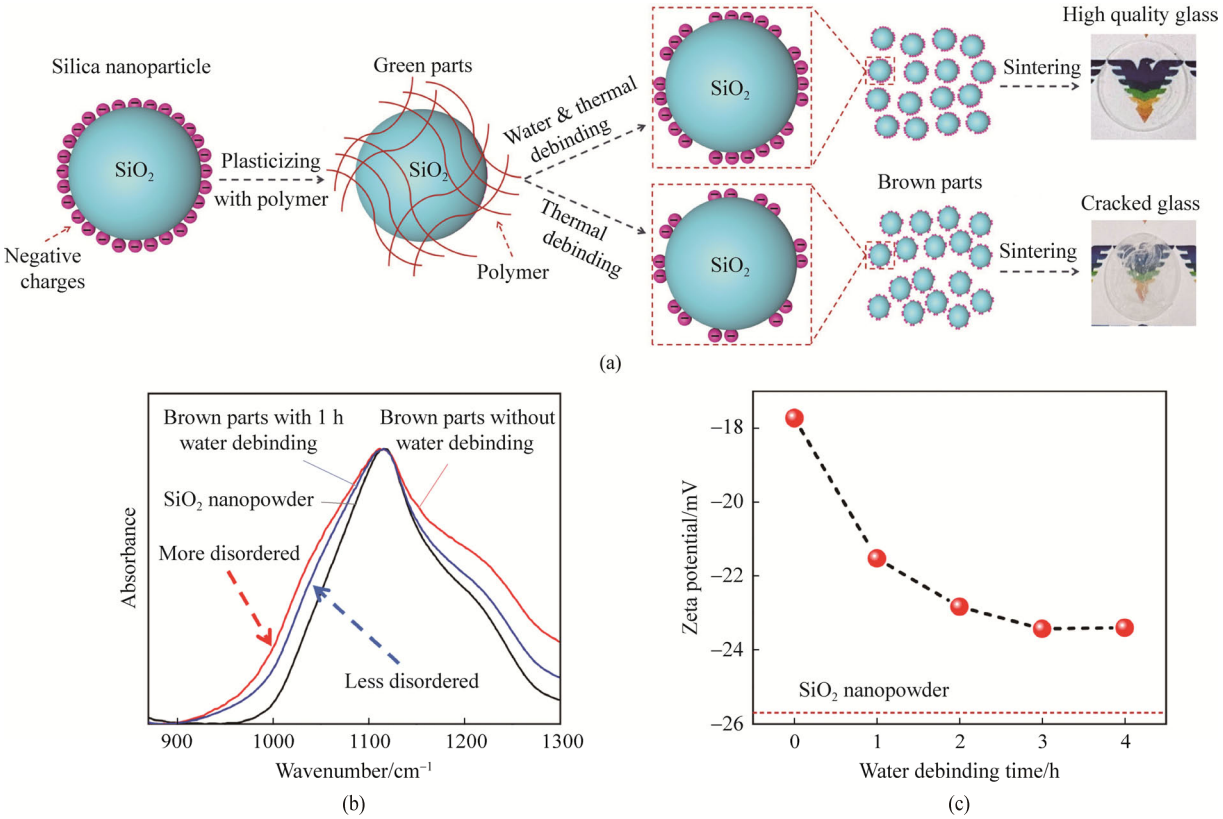


Fig. 5 (a) Schematic illustration for the change in the surface charge and the packing of silica nanoparticles after water and/or thermal debinding; (b) FTIR spectra of the silica nanopowders and the as-prepared brown parts with/without water debinding; (c) Zeta potential values of the as prepared brown parts obtained at different water debinding durations [45]

Interestingly, the surface charge and the molecular structure ordering of silica nanoparticles in the brown part became close to that of the silica nanopowder after performing water and thermal debinding for the green part [47]. These observations suggest the formation high-quality injection-molded silica glass after water debinding. Generally, this study confirmed the importance of water debinding step for the fabrication of high-quality silica glass *via* IM/sintering technique and examined the role of water debinding on the improvement of glass quality [45, 47].

3 Injection-molded PiSG for photonic applications

3.1 PiSG spectral converters for high-power and stable LEDs:

Due to the high-transparency of silica glass in Vis-NIR spectral regions, along with the high-chemical and thermal stabilities and high-hardness, such glass is regarded as an excellent host for efficient phosphors [31]. The embedding of phosphors particles into silica glass enabled the formation of stable and efficient PiSG spectral converters, which were used for the fabrication of high-power and stable LEDs [35]. Since pure silica glass was fabricated at low temperatures (< 1300 ℃) based on the IM technique, several oxide phosphors were incorporated into glass without interacting with silica during sintering. Owing to the importance of PiSG color converters for lighting and bioimaging applications, different luminescent phosphor particles have been incorporated into the injection-molded silica glass [31–35]. In this section, we discuss the recent progress in the fabrication of PiSG *via* IM/sintering technique. In 2024, Moushira, *et al* fabricated the first PiSG spectral converter *via* IM/sintering technique. They mixed the most efficient and stable $Y_3Al_5O_{12}:Ce^{3+}$ (YAG:Ce) phosphor powder together with PEG, PVB, and silica nanopowder in order to prepare silica-YAG:Ce-thermoplastic feedstock. YAG:Ce has been widely served as a spectral converter for the manufacture of high-power white LEDs (wLEDs) [33]. After plasticizing and molding (@ 130 ℃) the silica-YAG:Ce-thermoplastic mixture followed by debinding (@ 600 ℃) and sintering (@ 1150 ℃), luminescent YAG:Ce-PiSG was obtained as shown in Fig. 6a. To avoid the conversion of Ce^{3+} into Ce^{4+}, which leads to the reduction in IQE of YAG:Ce, the sintering process was performed under H_2/N_2 gas. After polishing the PiSG and decreasing the sample thickness to 0.3 mm, the PiSG spectral converters became transparent, and the transparency gradually decreased with increasing the content of YAG:Ce in PiSG as shown in Fig. 6b.

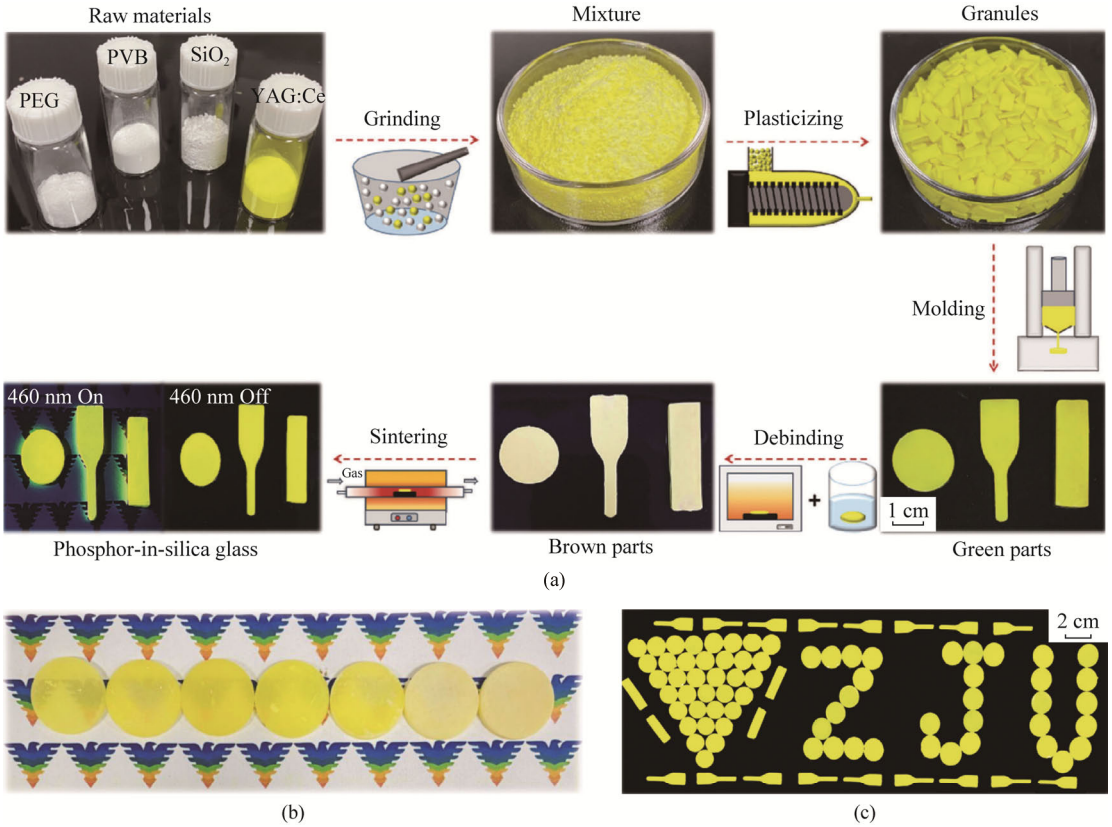


Fig. 6 (a) Schematic illustration for the fabrication of YAG:Ce-PiSG *via* IM/sintering technique; (b) Photograph of the injection-molded YAG:Ce-PiSG (0.3 mm thickness) at different YAG:Ce loadings starting from 10% (left) to 70% (in mass fraction) (right); (c) Photograph of 90 pieces of the injection-molded YAG:Ce-PiSG (10%, in mass fraction), showing the capability of high-throughput fabrication of PiSG *via* IM/sintering technique [33]

They molded 90 pieces of green parts made of silica-YA:Ce-thermoplastic with different shapes within 7.5 min with a cycle time of 5 s/piece, which is easily converted into YAG:Ce-PiSG after debinding and sintering processes as shown in Fig. 6c. The results of this study confirm the high-throughput manufacturing of YAG:Ce-PiSG *via* IM/sintering technique, which is needed for mass production of high-power LEDs [19, 33]. In this report, the structure, luminescence, and stability of the injection-molded YAG:Ce-PiSG spectral converter were examined by X-ray diffraction (XRD), SEM/energy-dispersive X-ray spectroscopy (EDS), photoluminescence (PL)/PL excitation (PLE), IQE, temperature-dependent PL, and chemical durability measurements. Briefly, the XRD and SED/EDS data (Fig. 7a, Fig. 7b) suggested that the YAG:Ce particles are preserved and the interfacial interaction between YAG:Ce and silica network is well inhibited during sintering process [31–35, 42].

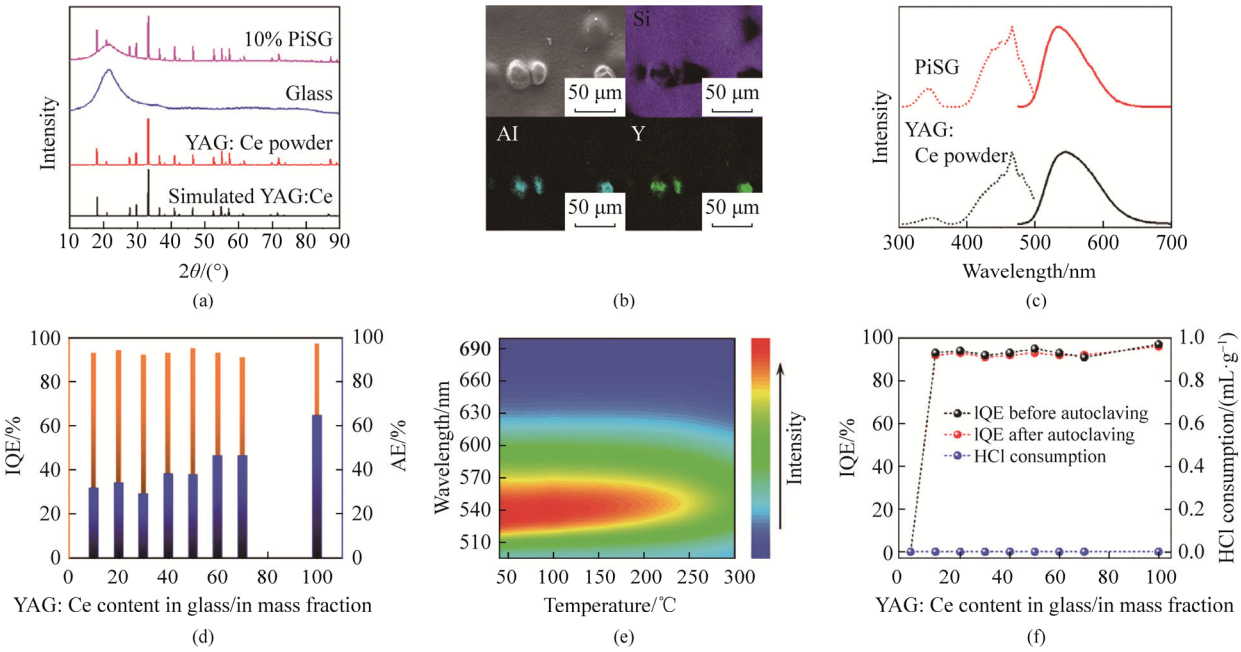


Fig. 7 (a) XRD patterns of the injection-molded silica glass and YAG:Ce-PiSG compared with simulated YAG:Ce pattern; (b) SEM/EDS mapping of the injection-molded YAG:Ce-PiSG; (c) PLE (dashed line) and PL (solid line) spectra of the YAG:Ce-PiSG and YAG:Ce powder; (d) IQE of the YAG:Ce powder and YAG:Ce-PiSG at different content of YAG:Ce; (e) A contour plot of the temperature-dependent PL spectra for the YAG:Ce-PiSG; (f) HCl consumption per gram and IQE before/after autoclaving in water for the YAG:Ce-PiSG at different YAG:Ce content [33]

In addition, the XRD patterns of the PiSG didn't show any diffraction peaks related to secondary phases and the SEM/EDS mapping showed YAG:Ce micro-particles were homogeneously distributed within silica network [33–35]. Consequently, the YAG:Ce-PiSG exhibited comparable PL/PLE spectra and IQE value to that of the YAG:Ce powder as shown in Fig. 7c, Fig. 7d. Furthermore, the YAG:Ce-PiSG illustrated excellent thermal and chemical stabilities (Fig. 7e, Fig. 7f), retaining its structure and luminescence efficiency (IQE > 90%) after autoclaving in water at high-temperature and high-pressure or even after heating the YAG:Ce-PiSG up to 200 ℃, showing the high PL thermal stability at high-temperature.

To enable YAG:Ce-PiSG for lighting applications, a high-power wLED (10 W) was fabricated in this work using the injection-molded YAG:Ce-PiSG as shown in Fig. 8a, Fig. 8b. The luminous efficiency (LE), correlated-color-temperature (CCT), and color-rendering-index (R_a) of the wLED device were improved by covering a layer of commercial $CaAlSiN_3:Eu^{2+}$ (CASN:Eu) red phosphor-in-silicone resin (CASN:Eu-PiS) on the surface of YAG:Ce-PiSG (Fig. 8a) [32–33]. They used CASN:Eu-PiS in the fabrication of wLEDs because of the difficulty of fabricating PiSG based on CASN:Eu. This is because the low structural stability of CASN:Eu during sintering, which is easily oxidized, losing its high IQE. The as-fabricated wLED based on YAG:Ce-PiSG/PiS-CASN:Eu demonstrated warm white light with a LE = 107 Im/W, CCT = 4161 K, and R_a = 90.7 at 50 mA as shown in Fig. 8a, Fig.8c. These results indicated that the as-fabricated injection-molded YAG:Ce-PiSG could be a promising spectral converter for high-power wLEDs [31–33]. Compared with the fabricated wLED devices using the expensive YAG:Ce single crystal or transparent ceramics, it is possible to fabricate stable and high-power wLEDs with a lower cost by incorporating YAG:Ce phosphor into chemically and thermally stable silica glass [33, 40–41].

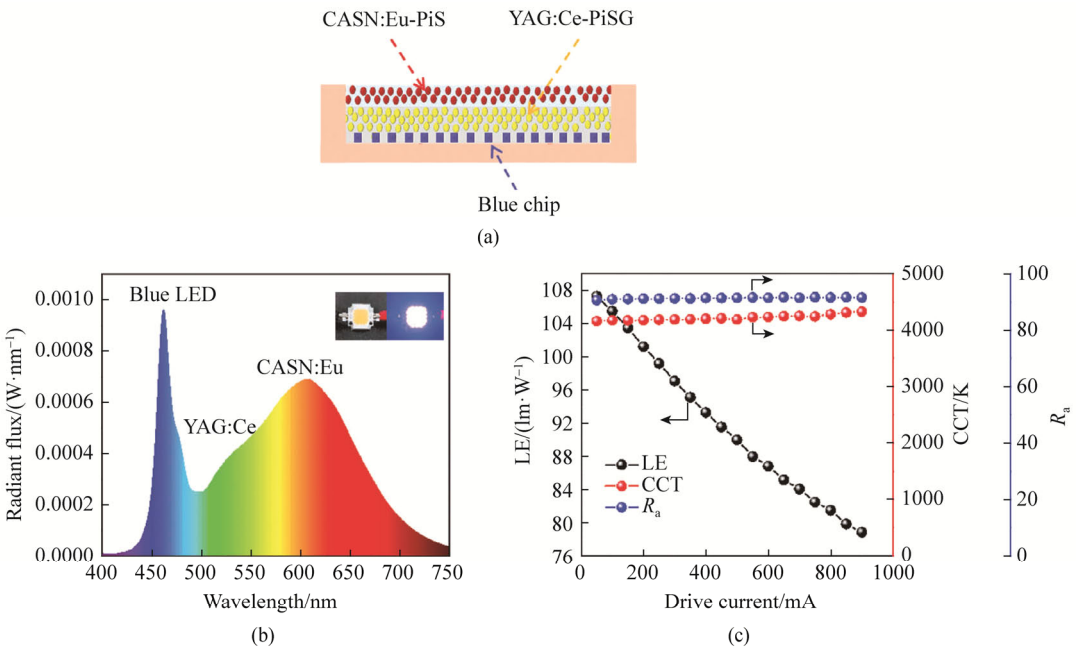


Fig. 8　(a) Schematic illustration for the as-constructed wLEDs device fabricated using YAG:Ce-PiSG/CASN:Eu-PiS; (b) Electroluminescence spectrum at 50 mA and (c) the LE, CCT, and R_a values as a function of the drive current for the as-fabricated wLEDs based on YAG:Ce-PiSG/CASN:Eu-PiS [33]

Despite the as-fabricated high-power wLEDs based on the injection-molded YAG:Ce-PiSG spectral converter showed high LE and R_a values, low chemically durable CASN:Eu-PiS has been utilized to improve the optical performance, which reduced the stability of the device. While, the PL spectra of the as-fabricated wLED covers only the visible spectral region (*i.e.*, 400–700 nm). Therefore, the IM/sintering technique was developed to fabricate PiSG containing efficient yellow, red, and NIR-emitting phosphors, improving the stability and extending the spectral range of LEDs device [34]. In 2025, Moushira *et al*. employed the IM/sintering technique to manufacture transparent PiSG spectral converters containing yellow-emitting YAG:Ce phosphor, red-emitting $Mg_2Al_4Si_5O_{18}:Eu^{2+}$ (MAS:Eu) phosphor, NIR-emitting YAG:Cr phosphor, and a mixture of YAG:Ce/MAS:Eu/YAG:Cr phosphors as shown in Fig. 9a [34]. The fabrication of PiSG using YAG:Ce/MAS:Eu/YAG:Cr phosphors exhibited the formation of efficient and stable color converters, with PL spectra covering the Vis-NIR spectral regions (*i.e.*, 400–900 nm) as shown in Fig. 9b. In addition, structural characterizations confirmed the inhibiting of phosphor-phosphor or phosphor-glass interfacial interactions during sintering at 1200 ℃. Moreover, the injection-molded PiSG spectral converters demonstrated high IQE (> 85%) and high-chemical/thermal stabilities, retaining more than 90% of its emission intensity at 200 ℃ as shown in Fig. 9c [31–32]. Consequently, the fabrication of PiSG using a phosphor mixture enabled the first construction of stable, high-power, and broadband LEDs device based on phosphor mixture-PiSG (Fig. 9d–Fig.9f). The as-constructed broadband LEDs based on PiSG (Fig. 9e) illustrated an excellent luminescence performance, *i.e.*, LE = 115 lm/W, CCT = 4531 K, and R_a = 90.1 at 50 mA.

Compared with the fabricated LEDs using YAG:Ce-PiSG (Fig. 9f), the incorporation of red-emitting MAS:Eu phosphor and NIR-emitting YAG:Cr phosphor together with yellow-emitting YAG:Ce phosphor into silica glass extends the luminescence spectral range of LEDs up to NIR region. Since the as-fabricated Vis-NIR-LEDs based on PiSG could emit both white and NIR light with high-power and high-color purity, the color-rendering capability of the as-fabricated pc-Vis-NIR-LEDs was further demonstrated by the photographs of cakes captured under the illumination with the manufactured light source (Fig. 9g). Additionally, by irradiating the human hand by the as-fabricated Vis-NIR-LEDs, a clear black-and-white photograph is taken for the hand veins using a night-vision camera (Fig. 9g). These proof-of-concept demonstrations disclosed the advantages of the as-fabricated Vis-NIR-LEDs based on phosphor mixture-PiSG in generating a high-power and broadband Vis-NIR light with high efficiency and manifest their great potential for applications from lighting to biological imaging applications [33–34]. This work suggests that the IM/sintering technique can be employed for high-throughput production of PiSG spectral converters containing a mixture of phosphors and thus enables the fabrication of stable and high-power broadband LEDs with a low cost and outstanding optical properties for lighting and bioimaging applications.

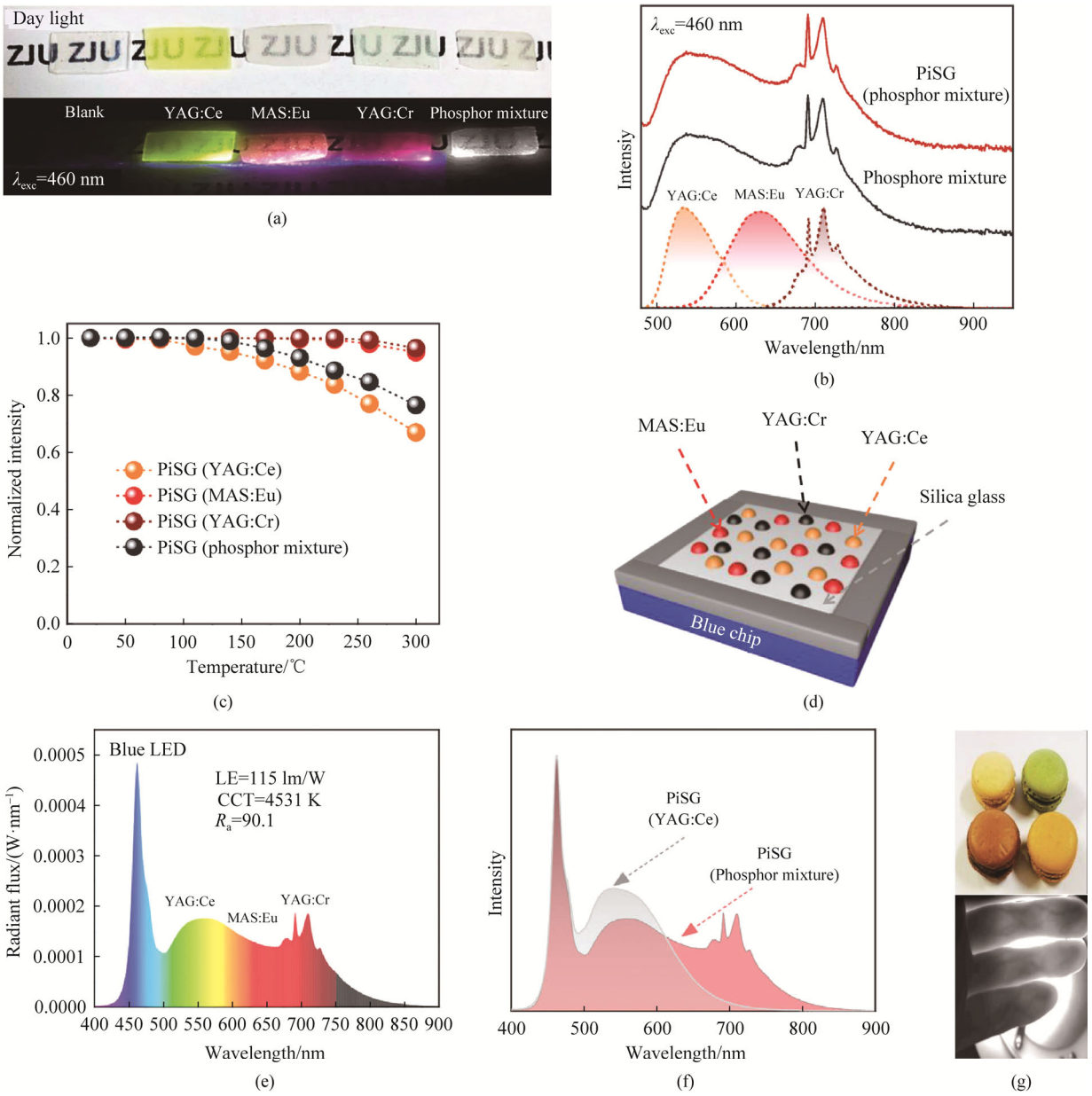


Fig. 9 (a) Photograph of the injection-molded PiSG using different type of phosphor powders taken under illumination of daylight and UV light (460 nm); (b) PL spectra and (c) temperature-dependent integrated emission intensity of the PiSG containing different type of phosphors; (d) Schematic illustration and (e) electroluminescence spectrum for the fabricated 10 W broadband Vis-NIR-LEDs based on PiSG containing phosphor mixture; (f) Electroluminescence spectra for the fabricated LEDs based on PiSG containing YAG:Ce and phosphor mixture; (g) Photographs of cakes (left) and hand veins (right) taken under the illumination with the as-fabricated Vis-NIR-LED based on PiSG (phosphor mixture), which were taken by a digital camera and a night vision camera, respectively [34]

3.2 Long persistent luminescent materials based on PiSG

The high-throughput fabrication of PiSG *via* IM/sintering process was not limited to luminescent phosphors for LED applications, but also it was employed to produce persistent PiSG (PPiSG) [35]. Long PPs possess the unique ability to store light energy and emit long-lasting afterglow, ranging from seconds to weeks after excitation ceases [48]. PPs exhibit luminescence across UV to NIR spectral regions with an afterglow duration. These materials hold a great promise for diverse applications, including security encryption, road signaling, decorative lighting, fluorescent lamps, data storage, sensing, anti-counterfeiting, and bioimaging [49]. Among PPs, oxide-based PPs (*e.g.*, silicates, aluminates, *etc*) were characterized by their superior chemical and thermal stabilities, along with extended afterglow performance [48–49]. However, integrating oxide-based PPs into transparent bulk materials with customizable shapes was proven challenging. Previous attempts using organic

polymers or low-melting inorganic glasses (< 1000 ℃) as the host networks for PPs suffer from poor chemical robustness, particularly in aqueous environments [49]. Conversely, incorporation of PPs into high-temperature glass melts (> 1300 ℃) often degrades their persistent luminescence due to strong interfacial interactions between the phosphor particles and the glass matrix. For commercial applications, PPs must be produced as monolithic, transparent forms with efficient luminescence, ultralong afterglow, high-thermal/chemical stabilities, and mechanical hardness [19, 33–35]. A promising solution is to incorporate the stable inorganic PPs into pure silica glass, which offers exceptional durability and transparency. High-throughput fabrication of translucent PPiSG in different shapes could meet market demands by combining the long afterglow of phosphors with silica glass's robustness [33–35]. To fabricate PPiSG, researchers have developed the IM/sintering technique, which successfully incorporates oxide-based PPs into silica glass without structural deformation.

In 2025, Moushira *et al*. demonstrated the IM/sintering technique using commercial blue-emitting $Sr_2MgSi_2O_7:Eu^{2+};Dy^{3+}$, green-emitting $SrAl_2O_4:Eu^{2+};Dy^{3+}$, and red-emitting $Y_2O_2S:Eu^{3+};Mg^{2+};Ti^{4+}$ PPs as raw materials for PPiSG fabrication (Fig. 10a) [35]. After molding followed by debinding process, the brown parts

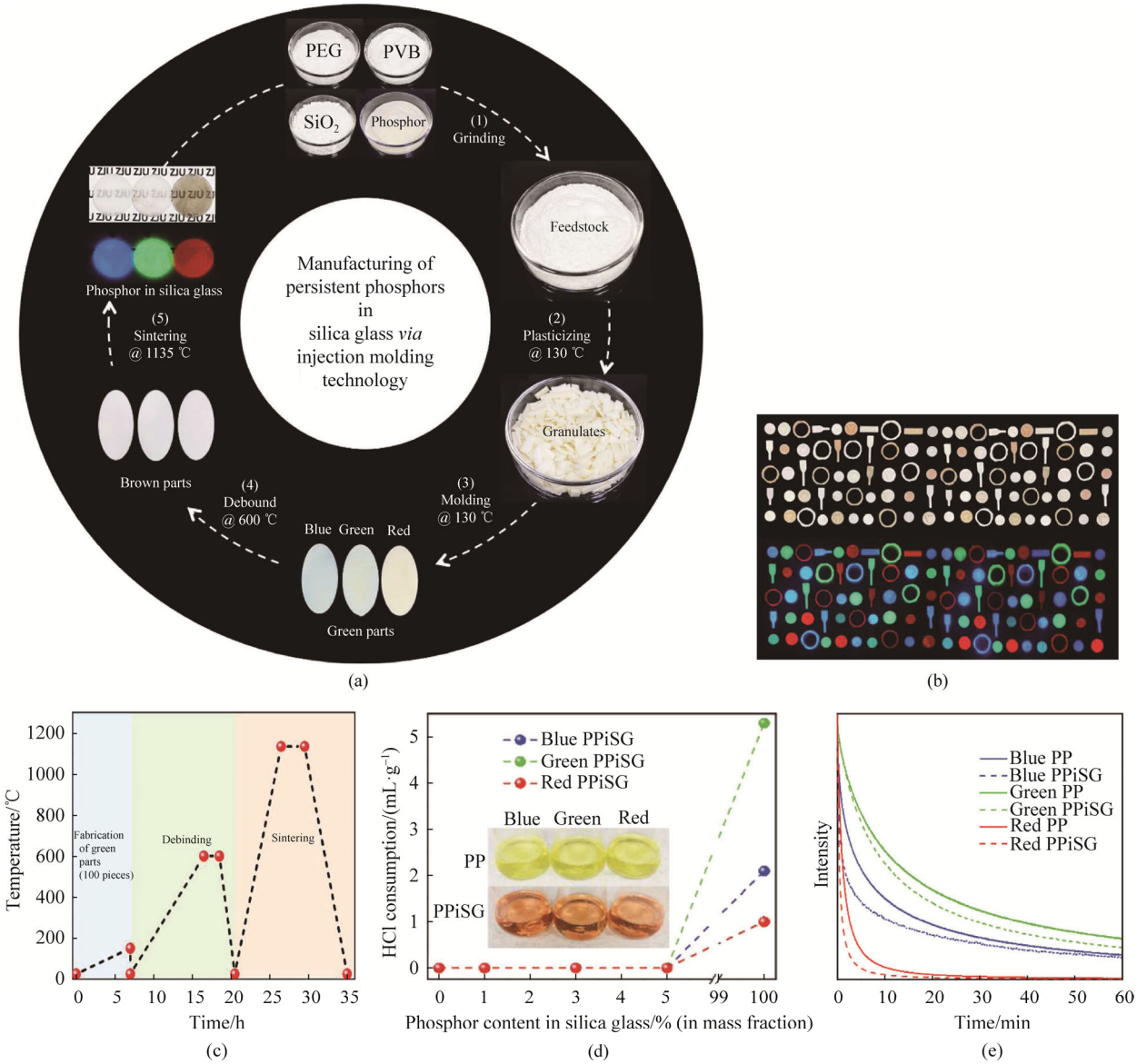


Fig. 10　(a) Schematic illustration for the fabrication of injection-molded PPiSG using different type of blue, green, and red PP powders; (b) Photograph of 100 pieces of the centimeter-sized blue, green, and red PPiSG fabricated by the IM/sintering technique, under daylight illumination (up) and after ceasing the illumination of UV light (down); (c) Temperature-time protocol for the fabrication of 100 samples of injection-molded PPiSG; (d) HCl consumption per gram after heat-treatment in water (@ 135 ℃) for the PP powders and the as-fabricated PPiSG at different loadings of PP; The insets are the photographs of the extracted solutions from the PP powders (up) and PPiSG (down) after autoclaving, confirming the high-chemical robustness of PPiSG; (e) Afterglow luminescence decay curves of the PPiSG and PP powders [35]

were densified into transparent multicolor PPiSG samples at 1135 ℃ as shown in Fig. 10a. The structural investigations by XRD, Raman, and SEM/EDS measurements confirmed that the PP particles were preserved during sintering process, retaining their luminescence properties. In this work, they fabricated different 3D shapes of multicolor PPiSG with blue, green, and red emissions and high-productivity (Fig. 10b). For example, 100 pieces of multicolor PPiSG were fabricated within 35 h, including the durations of green parts preparation and debinding/sintering processes (Fig. 10c) [19, 33]. Regarding the stability of multicolor PPiSG, the chemical durability test demonstrated that the stability of PP particles was improved after the incorporation into silica glass, showing ultrahigh-chemical durability compared with the PP powders as shown in Fig. 10d [31, 33–34]. Finally, the authors examined the optical properties of the as-fabricated multicolor PPiSG. Based on their investigations, the as-fabricated PPiSG possessed comparable afterglow luminescence decay performance compared with the raw PP powders as shown in Fig. 10e. In summary, the development of injection-molded and centimeter-sized PPiSG composites featuring multicolor emissions, long afterglow luminescence, high-stability, scalable production, and shape versatility, marked a significant breakthrough in persistent luminescence materials [49]. These advanced materials showed tremendous potential for diverse applications, including security encryption, data storage, optical sensing, bioimaging, and beyond [35, 48–49]. As demonstrated in this review, the high-throughput fabrication of PiSG through IM/sintering technique yields crystal-glass composites with exceptional optical and physicochemical properties. These exceptional properties make PiSG composites highly promising materials for photonic applications [4].

4 Summary and future perspectives

In this review, we have discussed the latest developments in the production of tailored injection-molded silica glass and PiSG products with intricate geometries for numerous applications. Transparent and complex-structured silica glass has been fabricated using the energy-efficient and cost-effective AM/sintering techniques. The shaping process of silica-polymer nanocomposite can be performed usually using AM techniques, including DIW, origami, FDM, SLA, TPL, μCAL. After a series of debinding and sintering processes at low temperatures, the green bodies are easily converted into transparent silica glass with high-quality and high-precision. Similar to silica glass, transparent PiSG spectral converters are also fabricated at low sintering temperatures *via* AM techniques, *e.g.*, SLA/sintering. The main drawback of the fabrication of silica glass and PiSG by AM/sintering techniques is that the printing is time-consuming, making these techniques unsuitable for large scale production. In order to solve the productivity issue for the fabrication of silica glass and PiSG, researchers have developed an AM method, *e.g.*, classical IM technology, which can be used in the fabrication of these materials. IM technique is characterized by high-throughput and low cost, which is needed for large scale industry. As discussed in this review, transparent silica glass and PiSG have been fabricated with high-productivity using IM/sintering technique. Using such approach, the rapid shaping of thermoplastic nanocomposites containing amorphous nanoparticles was performed by injecting the nanocomposite melt into different molds containing complex drilled structures. The molding rate can be as high as 5 s/piece, which was significantly faster than that required for the shaping of nanocomposite using other AM techniques. After water/thermal debinding followed by sintering at low temperatures, the green bodies containing silica or silica/phosphor mixture were densified into transparent silica glass or PiSG, respectively. Furthermore, it has been reported that the water debinding process is essential to improve the quality of the sintered silica glass. This is because the water debinding process reduces the amount of decomposed polymer and improves the packing of silica nanoparticles in the brown part through increasing the surface charge and molecular ordering of nanoparticles. Using this technique, researchers have successfully fabricated microfluidic chips and microlens as well as centimeter-sized luminescent silica glass through doping the glass network by active centers. In addition, different types of luminescent phosphors were incorporated into silica glass, forming efficient and stable PiSG, which was utilized for the fabrication of high-power Vis-NIR-LEDs. These results suggest that the injection-molded silica glass and PiSG are promising materials for various applications, *e.g.*, microfluidic, optics, lighting, and bioimaging.

Although the significant progress made in producing silica glass and PiSG with tailored geometries, several critical challenges remain that must be addressed in the near future. Firstly, it seems that the IM/sintering technique is limited for the fabrication of silica glass; the fabrication of injection-molded multicomponent silicate glasses has not been reported so far. This limitation arises from the restricted availability of raw materials, such as amorphous glass nanoparticles other than silica. More effort should be devoted to develop novel multicomponent nanopowders and thus extend the glass families that can be fabricated *via* the IM/sintering technique. Secondly, the emission spectrum of the as-fabricated injection-molded PiSG color converter covers only the 500–850 nm spectral region. In order to extend the spectral region of LEDs device, *i.e.*, 500–1500 nm, different NIR phosphor particles (*e.g.*, gallates phosphor) should be incorporated into glass network to obtain efficient and stable crystal-glass composites that can be served as color converters for the

fabrication of high-power and long lifetime NIR-LEDs and broadband Vis-NIR-LEDs. These NIR phosphors should possess high NIR-IQE under blue light, stable during sintering at high-temperature like YAG and MAS phosphors, and has a comparable refractive index to silica glass to reduce the scattering effect. Therefore, more systematic work should be performed in the future to optimize all of these parameters and to fabricate injection-molded multicomponent glasses and spectral converters for ultra-broadband LEDs.

References:

[1] BANSAL N P, DOREMUS R H. Handbook of Glass Properties[M]. Amsterdam: Elsevier, 1986.

[2] VARSHNEYA A K, MAURO J C. Fundamentals of inorganic glass making[M]//Fundamentals of Inorganic Glasses. Amsterdam: Elsevier, 2019: 631–685.

[3] MAURO J C, ELLISON A J, PYE L D. Glass: The nanotechnology connection[J]. Int J Appl Glass Sci, 2013, 4(2): 64–75.

[4] IKUSHIMA A J, FUJIWARA T, SAITO K. Silica glass: A material for photonics[J]. J Appl Phys, 2000, 88(3): 1201–1213.

[5] HENCH L L, DAY D E, HÖLAND W, et al. Glass and medicine[J]. Int J Appl Glass Sci, 2010, 1(1): 104–117.

[6] SCHMITZ A, KAMIŃSKI J, MARIA SCALET B, et al. Energy consumption and CO_2 emissions of the European glass industry[J]. Energy Policy, 2011, 39(1): 142–155.

[7] WINTOUR N. The glass industry: Recent trends and changes in working conditions and employment relations[R]. International Labour Office, 2015.

[8] LUO J J, HOSTETLER J M, GILBERT L, et al. Additive manufacturing of transparent fused quartz[J]. Opt Eng, 2018, 57(4): 1.

[9] KLOCKE F, DAMBON O, LIU G, et al. Analysis of wear of fused silica moulding using glassy carbon moulds[J]. Prod Eng Res Devel, 2016, 10(4–5): 367–374.

[10] KONSTANTINOVA T G, ANDRONIC M M, BAKLYKOV D A, et al. Deep multilevel wet etching of fused silica glass microstructures in BOE solution[J]. Sci Rep, 2023, 13(1): 5228.

[11] LIU X F, YANG Y T, QIU J R. Emerging techniques for customized fabrication of glass[J]. J Non Cryst Solids X, 2022, 15: 100114.

[12] XIN C X, LI Z, HAO L, et al. A comprehensive review on additive manufacturing of glass: Recent progress and future outlook[J]. Mater Des, 2023, 227: 111736.

[13] CHEN Y D, YE P R, HUANG L, et al. Photopolymerized 3D printing materials for optical elements[J]. Adv Opt Mater, 2024, 12(13): 2302685.

[14] KOTZ F, PLEWA K, BAUER W, et al. Liquid glass: A facile soft replication method for structuring glass[J]. Adv Mater, 2016, 28(23): 4646–4650.

[15] NGUYEN D T, MEYERS C, YEE T D, et al. 3D-printed transparent glass[J]. Adv Mater, 2017, 29(26): 1701181.

[16] KOTZ F, SCHNEIDER N, STRIEGEL A, et al. Glassomer: Processing fused silica glass like a polymer[J]. Adv Mater, 2018, 30(22): 1707100.

[17] XU Y, LI Y, ZHENG N, et al. Transparent origami glass[J]. Nat Commun, 2021, 12: 4261.

[18] MADER M, HAMBITZER L, SCHLAUTMANN P, et al. Melt-extrusion-based additive manufacturing of transparent fused silica glass[J]. Adv Sci, 2021, 8(23): 2103180.

[19] MADER M, SCHLATTER O, HECK B, et al. High-throughput injection molding of transparent fused silica glass[J]. Science, 2021, 372(6538): 182–186.

[20] KOTZ F, ARNOLD K, BAUER W, et al. Three-dimensional printing of transparent fused silica glass[J]. Nature, 2017, 544(7650): 337–339.

[21] WEN X W, ZHANG B Y, WANG W P, et al. 3D-printed silica with nanoscale resolution[J]. Nat Mater, 2021, 20(11): 1506–1511.

[22] TOOMBS J T, LUITZ M, COOK C C, et al. Volumetric additive manufacturing of silica glass with microscale computed axial lithography[J]. Science, 2022, 376(6590): 308–312.

[23] BAUER J, CROOK C, BALDACCHINI T. A sinterless, low-temperature route to 3D print nanoscale optical-grade glass[J]. Science, 2023, 380(6648): 960–966.

[24] LI M Z, YUE L, RAJAN A C, et al. Low-temperature 3D printing of transparent silica glass microstructures[J]. Sci Adv, 2023, 9(40): eadi2958.

[25] HUANG P H, LAAKSO M, EDINGER P, et al. Three-dimensional printing of silica glass with sub-micrometer resolution[J]. Nat Commun, 2023, 14: 3305.

[26] DESTINO J F, DUDUKOVIC N A, JOHNSON M A, et al. 3D printed optical quality silica and silica–titania glasses from sol–gel feedstocks[J]. Adv Mater Technol, 2018, 3(6): 1700323.

[27] DYLLA-SPEARS R, YEE T D, SASAN K, et al. 3D printed gradient index glass optics[J]. Sci Adv, 2020, 6(47): eabc7429.

[28] MOORE D G, BARBERA L, MASANIA K, et al. Three-dimensional printing of multicomponent glasses using phase-separating resins[J]. Nat Mater, 2020, 19(2): 212–217.

[29] PREDIGER R, KLUCK S, HAMBITZER L, et al. High-resolution structuring of silica-based nanocomposites for the fabrication of transparent multicomponent glasses with adjustable properties[J]. Adv Mater, 2024, 36(44): 2407630.

[30] LI B N, LI Z J, COOPERSTEIN I, et al. Additive manufacturing of transparent multi-component nanoporous glasses[J]. Adv Sci, 2023, 10(35): 2305775.

[31] ZHANG D, XIAO W G, LIU C, et al. Highly efficient phosphor-glass composites by pressureless sintering[J]. Nat Commun, 2020, 11(1): 2805.

[32] LI Q, XIAO W G, ZHANG D, et al. Phosphor-in-silica-glass: Filling the gap between low- and high-brightness solid-state lightings[J]. Laser Photonics Rev, 2022, 16(12): 2200553.

[33] MOHAMED M A, ALI M A, GUO S R, et al. High-throughput fabrication of phosphor-in-silica glass *via* injection molding[J]. Adv Opt Mater, 2024, 12(19): 2400323.

[34] MOHAMED M A, ALI M A, GUO S R, et al. Fabrication of a phosphor-in-silica glass spectral converter *via* injection molding for stable and high-power broadband LEDs[J]. Adv Opt Mater, 2025, 13(14): 2403434.

[35] MOHAMED M A, ALI M A, GUO S R, et al. Fabrication of translucent and chemically durable crystal-glass composite with multicolor persistent luminescence[J]. Adv Opt Mater, 2024, 12(21): 2400576.

[36] HARIYANI S, SÓJKA M, SETLUR A, et al. A guide to comprehensive phosphor discovery for solid-state lighting[J]. Nat Rev Mater, 2023, 8(11): 759–775.

[37] GUPTA I, SINGH S, BHAGWAN S, et al. Rare earth (RE) doped phosphors and their emerging applications: A review[J]. Ceram Int,

2021, 47(14): 19282–19303.
[38] ZHENG G J, LOU C J, YUAN Z Y, et al. Rare-metal-free ultrabroadband near-infrared phosphors[J]. Adv Mater, 2025, 37(4): 2415791.
[39] MA X G, LI X Y, LI J Q, et al. Pressureless glass crystallization of transparent yttrium aluminum garnet-based nanoceramics[J]. Nat Commun, 2018, 9(1): 1175.
[40] LATYNINA A, WATANABE M, INOMATA D, et al. Properties of Czochralski grown Ce, Gd: $Y_3Al_5O_{12}$ single crystal for white light-emitting diode[J]. J Alloys Compd, 2013, 553: 89–92.
[41] GONG M G, LIANG X J, WANG Y Y, et al. Novel synthesis and optical characterization of phosphor-converted WLED employing Ce: YAG-doped glass[J]. J Alloys Compd, 2016, 664: 125–132.
[42] ZHOU B Y, LUO W, LIU S, et al. Enhancing the performance of Ce: YAG phosphor-in-silica-glass by controlling interface reaction[J]. Acta Mater, 2017, 130: 289–296.
[43] CZEPIEL M, BAŃKOSZ M, SOBCZAK-KUPIEC A. Advanced injection molding methods: Review[J]. Materials, 2023, 16(17): 5802.
[44] BÄUMER D S. Handbook of Plastic Optics[M]. New York: John Wiley & Sons, 2010.
[45] GUO S R, ALI M A, MOHAMED M A, et al. Reduction of injection molded silica glass defects and enhancement of glass quality *via* water debinding[J]. Mater Chem Front, 2024, 8(5): 1400–1408.
[46] KOTZ F, RISCH P, ARNOLD K, et al. Fabrication of arbitrary three-dimensional suspended hollow microstructures in transparent fused silica glass[J]. Nat Commun, 2019, 10: 1439.
[47] ZHANG Q L, HU Y W, FENG Y W, et al. Critical role of water in fused silica glass by silica nanopowder sintering: Nanoparticle dispersion[J]. J Non Cryst Solids, 2023, 609: 122288.
[48] PAN Z W, LU Y Y, LIU F. Sunlight-activated long-persistent luminescence in the near-infrared from Cr^{3+}-doped zinc gallogermanates[J]. Nat Mater, 2011, 11(1): 58–63.
[49] LI Y, GECEVICIUS M, QIU J R. Long persistent phosphors: From fundamentals to applications[J]. Chem Soc Rev, 2016, 45(8): 2090–2136.

Recent Advances on Manufacture of Silica Glass and Phosphor-in-Silica Glass *via* Injection Molding

Moushira A MOHAMED[1], *Mohamed A ALI*[1], *LIU Xiaofeng*[2], *QIU Jianrong*[1]
(1. State Key Laboratory of Extreme Photonics and Instrumentation, College of Optical Science and Engineering, Zhejiang University, Hangzhou 310027, China; 2. School of Materials Science and Engineering, Zhejiang University, Hangzhou 310058, China)

Extended Abstract

Pure silica glass is a highly promising inorganic material for a range of applications in fields including microfluidics and photonics, owing to its remarkable characteristics, such as high transparency, stability, electrical insulation, and low thermal expansion. In the glass industry, large-sized pure silica glass is commonly produced using melting and quenching techniques, such as selective laser melting and precision glass molding methods. These traditional fabrication techniques suffer from the low producibility, difficulty to produce complex structures, as well as high energy consumption. To overcome such technical limitations, scientists developed the additive manufacturing (AM) techniques to easily shape and high-throughput fabricate silica glass at low temperatures. In their strategy, amorphous silica nanopowder is mixed with photopolymers or thermoplastics to obtain silica-organic nanocomposites with a high silica loading. Such hybrid composites are structured at low temperatures (< 150 ℃) *via* various AM technologies to obtain centimeter-sized or micro-sized green bodies with tailored shapes. Subsequently, the printed structures are densified into silica glass after a series of debinding and sintering processes at temperatures below 1300 ℃. Furthermore, the development of phosphor-in-silica glass (PiSG) led to the creation of spectral converters that combine the high luminescence efficiency of phosphors with the excellent chemical/thermal stabilities of silica glass, facilitating the production of high-power and stable light-emitting-diodes (LEDs). The manufacture of PiSG is often achieved using sophisticated and expensive high-pressure and high-vacuum techniques (*e.g.*, spark plasma sintering), which produce PiSG with a low productivity and limited shapes. In order to fabricate PiSG with customized shapes, AM/sintering technology was developed through incorporating the phosphor powder into silica-organic nanocomposites, which is transformed into translucent PiSG after sintering. Recently, transparent silica glass and PiSG with customized shapes were produced using AM/sintering methods. These innovative techniques allow for facile shaping and production of silica glass and PiSG at relatively low temperatures. Among AM/sintering techniques, injection molding (IM)/sintering method is characterized by its rapid molding, energy efficiency and cost-effectiveness, making it suitable for large-scale industrial production of silica glass and PiSG with intricate shapes and tailored sizes. It is interesting to note that the molding time of hybrid composite using IM equipment is much shorter than other AM technologies, which requires only 5 s to mold one piece. This makes IM technology promising approach for high-throughput fabrication of silica glass and PiSG.

This review focuses on the latest developments in the fabrication of silica glass and PiSG utilizing IM/sintering method. Additionally, we provide an overview for the potential applications of injection-molded silica glass and PiSG in the fields of microfluidics and photonics. At first, we highlight the detailed experimental procedures for the fabrication of silica glass *via* IM/sintering technology and how such technique succeeded in the manufacture of centimeter-sized and micro-sized silica glass with complex structures and high productivity. In addition, we discuss the influence of water debinding process on the quality of the

injection-molded silica glass. Water debinding serves a dual purpose: it enhances silica nanoparticle packing by augmenting surface charge and molecular order, and it minimizes the formation of micro-pores by reducing the volume of polymers available for decomposition during thermal debinding. This overall reduction in pore population facilitates the subsequent densification process during sintering. Afterwards, the development of IM/sintering for the manufacture of PiSG using different phosphor powders, *e.g.*, $Y_3Al_5O_{12}:Ce^{3+}$ (YAG:Ce), $Mg_2Al_4Si_5O_{18}:Eu^{2+}$ (MAS:Eu), $Y_3Al_5O_{12}:Cr^{3+}$ (YAG:Cr), and persistent phosphors, was discussed. The results showed that the interfacial interaction between phosphor particles and silica glass was well suppressed during sintering process and thus the luminescence performance of phosphor was retained in PiSG samples. Therefore, the PiSG spectral converters fabricated by IM followed by pressureless sintering exhibited a high luminescence efficiency, moderate transparency, and superior chemical and thermal stabilities. Furthermore, the fabrication of efficient and stable PiSG color converters by IM/sintering, enables the construction of high-power LEDs with long lifetime, covering the visible and near-infrared (NIR) spectral regions for lighting and bioimaging applications. This implies that IM/sintering technology may play a crucial role in the high-throughput fabrication of silica glass and PiSG that enables the production of cheap LEDs and microfluidic devices for numerous practical applications.

Summary and prospects While advances in fabricating tailored silica and PiSG geometries are notable, two critical challenges require immediate attention. The first limitation is the confinement of the IM/sintering technique to silica glass, as the production of multicomponent silicate glasses remains unreported. This bottleneck stems from a lack of commercially available amorphous nanoparticles for other glass compositions, underscoring the necessity for research into novel multicomponent nanopowders. The second challenge is the restricted spectral output of PiSG color converters, which currently only emit between 500–850 nm. Extending this range to 500–1500 nm for next-generation LEDs necessitates the incorporation of new NIR-emitting phosphors. Ideal candidates must exhibit high quantum efficiency and high thermal stability. Consequently, systematic research is essential to optimize these properties and realize injection-molded multicomponent glasses and ultra-broadband LEDs.

Kewords　silica glass; injection molding; phosphors; stable lighting equipment; solid-state lighting